Tel Aviv U. preprint TAUP-2444-97
March 1998

Kaon Radiative Decay $K^{\pm} \to \mu\nu\gamma$ at CKM at the Fermilab Main Injector

C. Milsténe[a], P. S. Cooper[b], M. A. Moinester[c]

[a] **On leave of absence at FNAL from TAU,**

caroline@fnal.gov

[b] **Fermi National Accelerator Laboratory,**

pcooper@fnal.gov

[c]**Tel Aviv University,**

murraym@silly.tau.ac.il

Presented by C. Milsténe at the Main Injector Workshop, Fermilab, May 1997.

Abstract

High statistics data for the $K^{\pm} \to \mu\nu\gamma$ decay can allow the precision determination of the kaon structure dependent form factors. This study is possible at the proposed FNAL CKM experiment. CKM (Charged Kaons at the Main injector) is a decay-in-flight spectrometer with two Ring Imaging detectors(RICH), and designed to run at the main injector with a high kaon flux. The radiative decay data might be taken complementary to the primary CKM effort to study the rare kaon decay ($K \to \pi\nu\bar{\nu}$) for which CKM was primarily designed. We summarize here the underlying physics of $K^{\pm} \to \mu^{\pm}\nu\gamma$, the experimental status, and how the CKM spectrometer may be adapted for this study.

I) Introduction

Data on the radiative decay $K^{\pm} \rightarrow \mu^{\pm}\nu\gamma$ can give important information on the properties of the hadronic weak currents of the $K^{\pm}$ meson. Chiral perturbation theory can be tested in such a process, since it is characterized by an effective chiral Lagrangian calculable in a low energy perturbative expansion. The amplitudes to $O(p^4)$ order for radiative semileptonic K decays can be determined from $K^{\pm} \rightarrow \mu^{\pm}\nu\gamma$ decay data.

The principal term of the decay is the Internal-Bremsstrahlung (IB) of charged particles, which is completely described by QED. The second term is the direct emission of the γ from the intermediate kaonic states; this term is structure dependent (SD). The direct emission of the right-handed and left-handed photon are mediated respectively by vector hadronic currents dependent on the vector form factor (F_V), and axial-vector hadronic currents dependent on the axial vector form factor (F_A). The cross-section of the structure dependent terms was first derived by Neville [1] as a function of these form factors. Since then, many calculations have given predictions on the values of the form factors. The values obtained are $\mid F_V \mid M_K$=0.06 to 0.8 and F_V/F_A=-0.97 to 0.58 [2, 3, 4, 5, 6, 7, 8, 9, 10, 11, 12, 13, 14].

Chiral Perturbation theory predicts to order $O(p^4)$ that the form factor ratio is given in terms of the combination of chiral coefficients $(L_9^r + L_{10}^r)$, with $F_V/F_A=32\pi^2(L_9^r + L_{10}^r)$. Also, the kaon electric polarizability to order $O(p^4)$ is expressed as $\alpha_K = (4\alpha_f/m_K F_K^2) * (L_9^r + L_{10}^r)$, where α_f is the fine structure constant and F_K is the Kaon decay constant. Therefore the polarizability is proportional to the ratio F_V/F_A, which may be measured in Kaon radiative decay experiments [15, 16].

The experimental measurements are generally given in terms of $\mid F_V - F_A \mid M_K$ for SD^- and the interference term (INT^-), and $\mid F_V + F_A \mid M_K$ for SD^+ and the interference term INT^+. These terms populate differently the Dalitz plot representing this three-body decay. The Dalitz plot population is very sensitive to the phase and size of the Structure Dependent terms ($SD^{\pm}$), ($INT^{\pm}$), as shown in Figure 1 Fig. 1.

It would have been sufficient to measure the interference term in the $K^{\pm} \rightarrow \mu^{\pm}\nu\gamma$ decay, but too few events are available for this decay. From a measurement of $SD^{\pm}$ alone, one only gets an ambiguous evaluation of F_V and F_A. In CKM, we plan to measure both the SD^- term and the INT^- term.

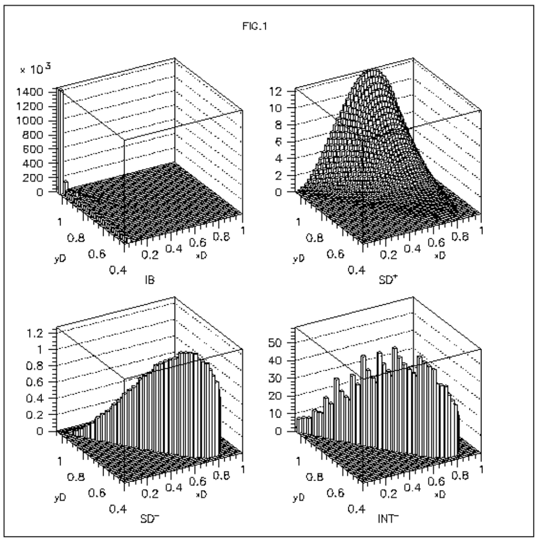

Figure 1: The Dalitz plot for each of the terms contributiong to the $K^{\pm} \rightarrow \mu\nu\gamma$ decay

We will describe the physics motivation in section II, the status of measurements in section III, FNAL E761 measurement attempts in section IV, the CKM possibilities in section V, and our conclusions in section VI.

II) Physics Motivation

There are three types of contribution to this kaon radiative decay. They are the Internal-Bremsstrahlung (IB), the structure dependent terms (SD) where the photon is emitted from intermediate Kaon hadronic states, and the interference terms between them (INT). The Feynman diagrams of the IB terms and the triangular diagrams of SD terms are represented in Figure 2 Fig. 2.

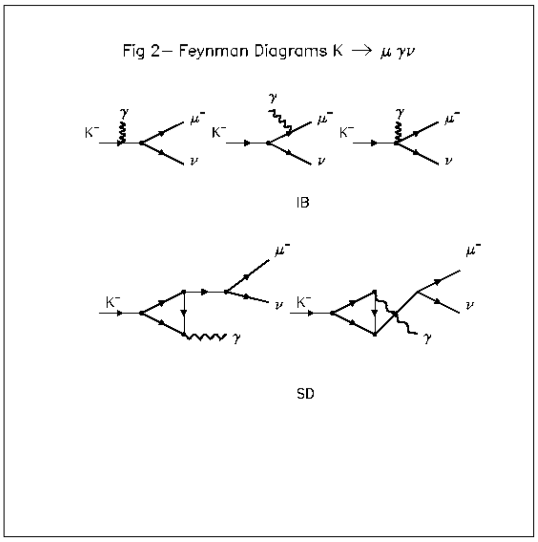

Figure 2: Feynman diagrams of the IB terms and the triangular diagrams of SD terms

In the SD terms, the radiative decay $K^{\pm} \to \mu^{\pm}\nu\gamma$ depends on the properties of the hadronic weak currents. There are no hadrons involved in the final state. Therefore, the kinematics of the three almost massless point-like particles emitted by the $K^{\pm}$ probes the internal structure of the kaon without final state interactions.

The amplitudes SD can be written in terms of F_V and F_A. There are two componants, SD^{+} proportional to $\mid F_V + F_A\mid^2$, and SD^{-} proportional to $\mid F_V - F_A\mid^2$. The SD^{+} and SD^{-} terms correspond to the emission of photons with positive and negative helicities, respectively. The interference term is composed of two terms, INT^{+} and INT^{-} which correspond to the interference of IB with SD^{+} and SD^{-} respectively [17, 18]. The interference terms allow a determination of the sign of the form factors, and thereby the sign of the amplitudes. The Dalitz plot expresses decay probability as a function of x (related to the γ energy) and y (related to the muon energy). Figure 1 Fig. 1 shows that the different terms populate different regions of the Dalitz plot.

The decay rate is then given as:

$$d^2\Gamma/dxdy = \Gamma(IB) + \Gamma(SD^+) + \Gamma(SD^-) + \Gamma(INT^+) + \Gamma(INT^-).$$

We have:

$$\begin{aligned}
\Gamma(IB) &= A_{IB} \bullet f_{IB}(x,y) \\
\Gamma(SD^+) &= A_{SD} \bullet f^+_{SD}(x,y) \bullet ((F_V + F_A) \bullet M)^2 \\
\Gamma(SD^-) &= A_{SD} \bullet f^-_{SD}(x,y) \bullet ((F_V - F_A) * M)^2 \\
\Gamma(INT^+) &= A_{INT} \bullet f^+_{INT}(x,y) \bullet ((F_V + F_A) \bullet M) \\
\Gamma(INT^-) &= A_{INT} \bullet f^-_{INT}(x,y) \bullet ((F_V - F_A) \bullet M).
\end{aligned}$$

Here, $\mathrm{A}_{IB} = \mathrm{W}^2_{K\mu} \bullet \frac{\alpha_f}{2\pi} \bullet \frac{1}{(1-r)^2}$

$\mathrm{A}_{SD} = \mathrm{A}_{IB} \bullet \frac{1}{4r} \bullet \frac{M_K^4}{F_K^2}$

$\mathrm{A}_{INT} = \mathrm{A}_{IB} \bullet \frac{M_K^2}{F_K}$

$\mathrm{W}^2_{K\mu}$ =0.6351 is the probabitlity for the decay $K^- \to \mu^- \nu$,

$x = \frac{2E_\gamma^{CM}}{M_K}$, $y = \frac{2E_\mu^{CM}}{M_K}$, $r = \frac{M_\mu^2}{M_K^2}$

$$f_{IB}(x,y) = \left(\frac{1-y+r}{x^2 \bullet (x+y-1-r)}\right) \bullet \left(x^2 + 2 \bullet (1-x) \bullet (1-r) - \frac{2 \bullet x \bullet r \bullet (1-r)}{x+y-1-r}\right)$$

$$f^+_{SD}(x,y) = [x+y-1-r] \bullet [(x+y-1) \bullet (1-x) - r]$$

$$f^-_{SD}(x,y) = [1-y+r] \bullet [(1-x)(1-y) + r]$$

$$f^+_{INT}(x,y) = \left(\frac{1-y+r}{x \bullet (x+y-1-r)}\right) \bullet [(1-x) \bullet (1-x-y) + r]$$

$$f^-_{INT}(x,y) = \left(\frac{1-y+r}{x \bullet (x+y-1-r)}\right) \bullet [x^2 - (1-x) \bullet (1-x-y) - r].$$

III) Experimental Status

Previous experiments with measurements of F_A and F_V are reported in Table 1 together with the predicitons from Chiral Perturbation theory [12, 14]. The theory value quoted for $\mid F_V + F_A|M_K$ is obtained using the $K^- \to e\nu\gamma$ decay data.

Predictions from Chiral Theory	$\mid F_V + F_A\mid M_K$=0.134	$\mid F_V - F_A\mid M_K$=0.049
CERN PS Experiment	$\mid F_V + F_A\mid_e M_K$= 0.153 $\pm$0.01	-2.5<$\mid F_V - F_A\mid_e M_K$ < 0.5
KEK Experiment	$\mid F_V + F_A\mid_\mu M_K$ <0.23	-2.5<$\mid F_V - F_A\mid_\mu M_K$ <0.3
ITEP PS Experiment	-1.2<$\mid F_V + F_A\mid_\mu M_K$ <1.1	-2.2<$\mid F_V - F_A\mid_\mu M_K$ <0.6
BNL 787 Experiment	$\mid F_V + F_A\mid_\mu M_K$ = 0.165$\pm$0.007$\pm$0.011	Not measured

Table 1: Theoretical Predictions and Experimental status

The Cern PS experiment $K^- \to e\nu\gamma$ was performed utilizing a stopped K- separated beam in a counter experiment, with a lead-glass detector for the γ [20]. They had 51 $\pm$ 3 events to determine SD^+ and 9 events to determine limits on SD^-. The KEK experiment $K^- \to \mu\nu\gamma$ used a High Resolution Spectrometer with a NaI(T1) γ detector and a stopped K- separated beam [17]. In the SD^+ region 3.44 events were obtained after fit, while in the SD^-+INT^- region, 142 events were measured. The ITEP-PS experiment $K^- \to \mu^-\nu\gamma$, used a 700-liter Xenon Bubble Chamber and stopped Kaon from a separated beam, with 442 $K^- \to \nu\mu\gamma$ candidates [21]. E761 attempted to measure $\mid F_V - F_A|M_K$, as described in E761 reports [18, 24]. The most recent value of $\mid F_V + F_A|M_K$ was measured with good precision using 2693 $K^- \to \mu^-\nu\gamma$ obtained at BNL with stopped kaons. Their result confirms the $K^- \to e^- \nu\gamma$ experimental value, (and universality), and they both confirm the predictions from Chiral theory [12, 13, 14]. They were also able to measure for the first time the Branching ratio BR(SD$^+$) of the order of 10^{-5} with a precision of the order of 20% [22, 23]. CKM will be sensitive to the SD$^-$ term, and should be able to get a precise measurement, including the sign of $(F_V - F_A)\ M_K$.

To summarize the present situation, a value was obtained from previous CERN and BNL data for $\mid F_V + F_A|M_K \approx 0.153 - 0.165$. For $\mid F_V - F_A|M_K$, the best limits from the different experiments are in the range [-2.2,+0.3] [17, 21].

IV) E761 Studies

The 375 GeV/c Hyperon unseparated beam with 5% K$^-$ and the E761 High Resolution Spectrometer in the cascade setup were used. The background to the $K^- \to \nu\mu\gamma$ channel comes from K decays with π^0. These decays have larger branching ratio than the γ channel, with $\pi^0 \to \gamma\gamma$ faking the $\nu\gamma$, e.g.

$$K^- \to \pi^-\pi^0 \quad ; \quad BR = (21.17 \pm 0.05)\%$$

$$K^- \to \pi^-\pi^0\pi^0 \quad ; \quad BR = (1.73 \pm 0.04)\%$$

$$K^- \to \mu\nu\pi^0 \quad ; \quad BR = (3.18 \pm 0.08)\%$$

$$K^- \to e\nu\pi^0 \quad ; \quad BR = (0.55 \pm 0.028)\%.$$

Backgrounds which come from the other Hyperons in the beam; (e.g., the decays $\bar{\Sigma}^- \to \bar{p}\pi^0$, $\Xi^- \to \Lambda\pi^-$) were removed by the analysis cuts. These cuts also removed part of the background coming from competing K$^-$ decays, e.g. $K^- \to e^-\nu\pi^0$ decay [24]. Other sources of background were the interactions of the beam in detector materials.

An E761 analysis [24] considered a partial sample of 2838 events. Taking into account the energy measured in the PbG detector and the position of the highest energy cluster, the components of the photon momentum were computed. The momentum resolution of the lead glass detector was ($\sigma P_\gamma/P_\gamma$=.033+.3276/$\sqrt{E}_\gamma$) and the angle precision was $\sigma\theta_\gamma$=0.66 mrad. The missing mass square to the neutrino was then computed, using the measured momentum of the incoming and charged outgoing particles, and also the momentum of the γ computed from the information in the PbG detector. The momentum resolutions of the incoming and the charged outgoing particle are better than for the γ and are reported in the table in the next paragraph. The particles are not identified.

Figure 3 Fig. 3 shows the square of the missing-mass, where the peak is rather wide due to the poor resolution in mass which comes from the poor resolution in the momenta used to calculate it.

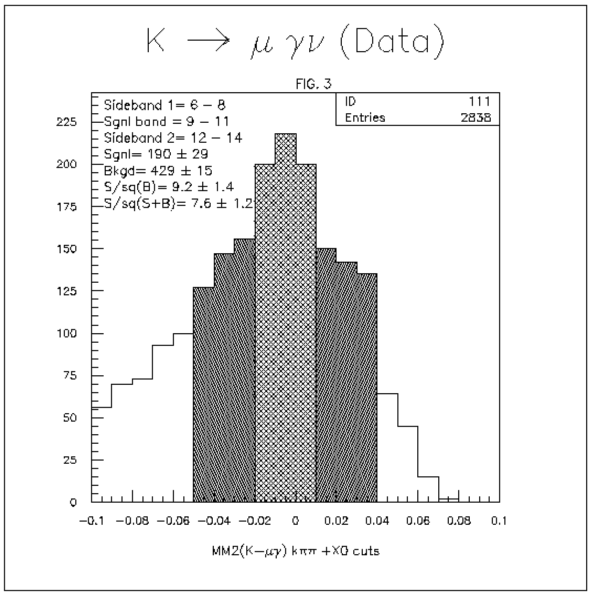

Figure 3: Side-bands background substraction in the square of the missin+ mass MM2(K-$\mu\gamma$)

In Figure 3 Fig. 3, one can see 2838 events. Considering a side-band background substraction, this can be separated into $\simeq$ 190$\pm$ 29 events located in a peak at 0 GeV, above a background of 429 $\pm$ 15 events.

The above summary shows that the signal to background ratio in E761 was not good enough to get quality data on the Kaon radiative decay. This is so because of the absence of μ identification, because of the limited γ detector resolution, and because the background from decays and interactions were very high compared to the signal.

V) Kaon radiative decay with CKM

1) We expect a 30 MHZ Kaon separated beam at the main injector. This will lead to: K^+ *Decay* $6MHZ$

$BR(K\mu\nu\gamma)$ $5.\bullet 10^-3$

Acceptance $1.\bullet 10^-2$

$\longrightarrow\longrightarrow\longrightarrow$

300 HZ

10^5 sec/week

$\longrightarrow\longrightarrow\longrightarrow\longrightarrow\longrightarrow\longrightarrow\longrightarrow$

30 Million events/week

Here we define 1 week = 100 beam-hours * 1000 sec/hour. Therefore, in one week, we expect the number of $K^- \rightarrow \nu\mu\gamma$ decays to be higher than all previous experiments together.

	E761 DATA	CKM MC
$\sigma P_K/P_K$	0.77%	0.24%
$\sigma P_\mu/P_\mu$	1.70%	0.78%
$\sigma P_\gamma/P_\gamma$	.033+.3276/$\sqrt{E}_\gamma$	0.01/$\sqrt{E}_\gamma$
$\sigma\theta_\mu$	28 μrad	124 μrad
$\sigma\theta_\gamma$	1.52 mrad-3.34*P_γ/P_K	0.66 mrad

Table 2: Resolution Comparison

2) The CKM apparatus is shown in Figure 4 Fig. 4. CKM [25] is built with two RICH detectors.

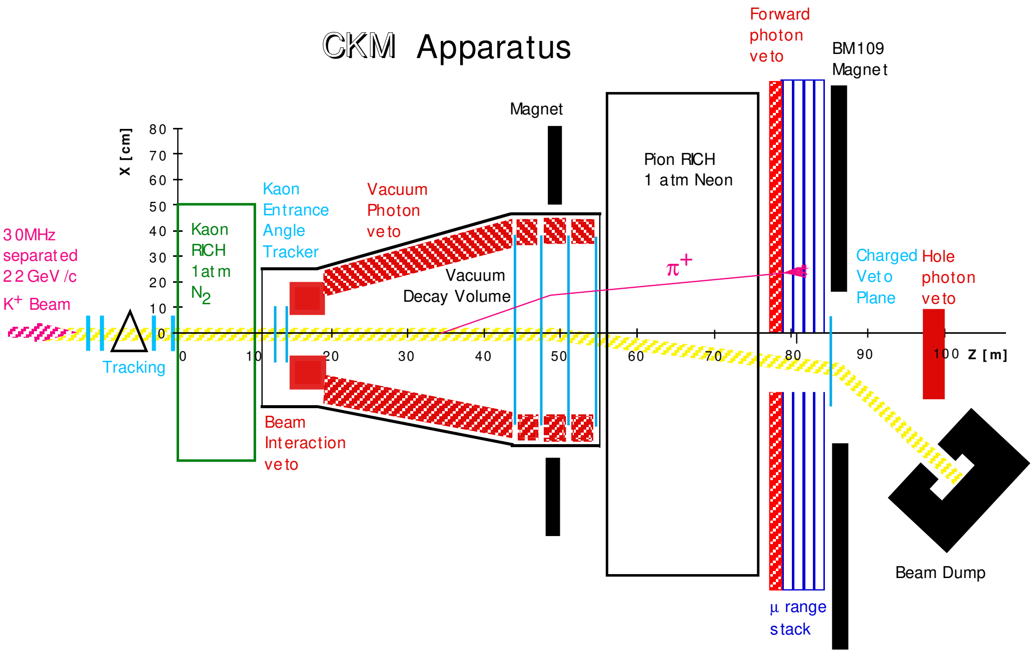

Figure 4: The CKM spectrometer

One is a RICH detector ten meters long at the threshold of the 22 GeV kaon beam; containing CF4 at 0.7 atm pressure. The second RICH is twenty meters long at the pion threshold; containing Neon at 1 atmosphere. Both RICH detectors are separated by a vacuum decay volume 30 meters long and covered by a γ veto layer. A PbG stack at the rear of the second RICH is an additional veto to clean the background. The PbG stack is followed by a μ range stack and a bending magnet to tilt the beam to the beam dump. An additional PbG stack located eighty meters from the entrance of the first RICH covers the central hole.

We have simulated the CKM system with a CsI γ detector of the KTEV variety added at the rear of the pion RICH and before the PbG veto stack, at about sixty meters from the entrance of the Kaon RICH. This γ detector will be 15 cm wide in the y direction and 70 cm wide in the x direction, and shifted by 10 cm from the center of the beam. Each of the 75 blocks of CsI will be 4x4 cm^2, as may be seen in Figure 4Fig. 4. In the CsI detector, a nitrogen laser similar to that used by KTEV is needed to calibrate the digital readout system [26]. This detector system also allows kaon identification in the Kaon RICH, as well as muon identification using the pion RICH and the μ range stack. Such information were not avalaible in E761. Together with the photon veto, the PbG stack, and the better resolution photon detector, CKM will achieve both a better identification of the events of interest and a better background rejection.

We compare the expected photon resolution of the CsI detector to the photon resolution achieved in E761. Those resolutions are obtained using the EXP Monte Carlo. The comparison is made with E761 data. Most of the comparative resolutions are reported below in Table 2.

3) We achieved with the E761 PbG detectors the following resolutions across the Dalitz plot:

$$\sigma x \simeq 0.3\ E761\ \ ;\ \sigma x \simeq 0.015\ \ CKM$$

$$\sigma y \simeq 0.05\ E761\ \ ;\ \sigma y \simeq 0.003\ \ CKM$$

The acceptance reached using the EXP [1] is of the order of 1% as used in the evaluation of the number of events one obtains in a week of CKM run. A plot of the Acceptance per bin across the Dalitz plot is represented in Figure 5 Fig. 5.

In that figure, the bin size is twice the resolution in x and y respectively (a 2σ margin was allowed). We generated 100,000 $K^- \to \nu\mu\gamma$ decays with EXP-MC. In Fig. 5, we show the percentage Acceptance across the Dalitz plot.

VI) Conclusion

In the Main injector, a week of CKM running will provide more $K^- \to \nu\mu\gamma$ than all previous experiments together. The background will be minimized,

[1]EXP is a fast Monte-Carlo written by P.S.Cooper which had had many lifes starting with a BNL/FNAL experiment and through e761 and e781 went over a new transformation for CKM

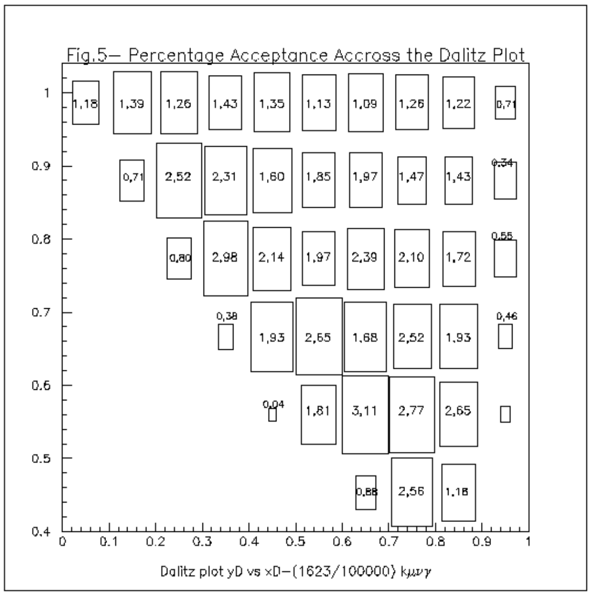

Figure 5: Percentage Acceptance accross the Dalitz plot,a total of 1623 + out of 100000 events were seen

considering the vacuum in the decay volume, the photon veto, and the PbG stacks. The events will be better identified, having both kaon and muon identification. The signal will be better measured for all the particles, especially the photons.

Acknowledgements

Special thanks are due to G. Burdmann, C. Quigg, for interesting discussions. Thanks are due to S. Kananov and A. Ocherashvili for help with the GEANT simulations of the E761 studies. This work was supported in part by the U.S.-

Israel Binational Science Foundation, (BSF), Jerusalem, Israel; and in part by A. Zaks to whom one of us is particularly thankful.

List of Tables

List of Figures

References

[1] D. E. Neville, Phys. Rev. 124, 2037, (1961).

[2] A. Q. Sarker, Phys. Rev. 173, 1749 (1968).

[3] W. K. Kummer, W. Majerotto, Nuovo Cimento 55, 558 (1968).

[4] R. Rockmore, Phys. Rev. 177, 2573 (1969).

[5] M. G. Smoes, Nucl. Phys. B20, 237 (1970).

[6] N. J. Carron, R. L. Schult, Phys. Rev. D1, 3171 (1970).

[7] K. A. Milton, W. W. Wada, Phys. Lett. 98B, 367 (1980).

[8] D. A. Bryman, P. Depommier, C. Leroy, Phys. Reports 88 (1982) 151.

[9] M. Pavers and M. D. Scadron, Nuovo Cimento 78A, 159 (1983).

[10] E. Z. Avakyan*et al.*, Dubna Preprint R2-86-441, (1986).

[11] J. Gasser and H. Leutwyler, Nucl. Phys. B250, 517 (1985).

[12] J.F. Donoghue, Preprint UMHEP-329-1990

[13] Ametller,*et al.*, Phys. Lett. B303, 140 (1993).

[14] J. Bijnens, G. Ecker, J. Gasser, Nucl. Phys. B396, 87 (1993).

[15] J. F. Donoghue, B. R. Holstein, Phys. Rev. D40, 2378 (1989)

[16] D. Babusci, S. Belluci, G. Giordano, G. Matone, A. M. Sandorfi, M. A. Moinester, Phys. Lett. B277, 158 (1992), and references therein.

[17] Y. Akiba *et al.*, Phys. Rev. D32, 2911 (1985).

[18] V. S. Demidov, M. A. Kubantsev, A. N. Nikitenko, ITEP Preprint ITEP-30-1993, E761 FNAL Report HNOTE 524.

[19] M. A. Moinester, Proceeding of the Workshop on Virtual Compton Scattering,Clermont-Ferrand,France,Edit.V.Breton,June1996,TelAviv Univ.Preprint, TAUP-2354-96, and references therein.

[20] J. Heintze *et al.*, Nucl. Phys. B149, 365 (1979)

[21] V. S. Demidov *et al.*, Sov. J. Nucl. Phys. 52, 1006 (1990)

[22] M. R. Convery, Princeton University, UMI-97-07305, Ph.D. Thesis (1996).

[23] M. R. Convery, Proceeding of the 1996 Minneapolis DPF Conference.

[24] P. S. Cooper and C. Milsténe, E761 FNAL Report HNOTE 685, V.S. Demidov, M.A.Kubantsev and A.N. Nikitenko,Preprint ITEP-30-1993, HNOTE 524.

[25] P. S. Cooper, Contribution to the Main Injector Workshop, Fermilab, May 1997.

[26] R. S. Kessler *et al.*, Nucl. Inst. Meth. A368, 653 (1996)